

<https://doi.org/10.1038/s43247-024-01502-8>

Glacial troughs as centres of organic carbon accumulation on the Norwegian continental margin

Check for updates

Markus Diesing ¹ ✉, Sarah Paradis ², Henning Jensen¹, Terje Thorsnes¹, Lilja Rún Bjarnadóttir¹ & Jochen Knies^{1,3}

The role of continental margin sediments in the carbon cycle and the associated management potential for climate mitigation are currently poorly understood. Previous work has indicated that margin sediments store significant amounts of organic carbon, but few studies have quantified the rates at which organic carbon is accumulated. Here, we use machine learning to make spatial predictions of the organic carbon stocks and accumulation rates of sediments on the Norwegian continental margin. We show that surface sediments (upper 10 cm) store 814 Tg and accumulate 6 Tg yr⁻¹ of organic carbon. Shelf-incised glacial troughs account for 39% of the stocks and 48% of the accumulation, with the main accumulation hotspot located in the Skagerrak. Continental margin sediments accumulate organic carbon at scales much larger than vegetated coastal ecosystems in Norway because of their larger extent. Future studies should explore to what extent management interventions could increase accumulation rates, e.g., by minimising anthropogenic disturbance of seafloor sediments.

The burial of carbon in seafloor sediments is crucial for moving carbon from the short-term surface to the long-term geological cycle¹. This long-term carbon cycle is, in turn, controlling the concentration of atmospheric carbon dioxide (CO₂) over geological timescales². The size of the organic carbon seafloor sink, and the relative contributions of the continental margins versus the deep-sea, have been a matter of research for the last 50 years or so. A first estimate, based on multiplying average organic carbon content of Holocene sediments by area and thickness, yielded 223 Tg C yr⁻¹, of which 10% and 88% are deposited on the continental shelf and slope, respectively³. Berner⁴ argued that organic carbon is preferentially buried in deltaic shelf sediments (83% of a total burial rate of 126 Tg C yr⁻¹). His estimates were subsequently revised by Hedges and Keil⁵ to account for organic carbon burial in sediments of the continental shelves and upper slopes, respectively, and estimated that roughly 90% of organic carbon is buried in coastal and continental margin settings. Routine collection of ocean colour data with satellites has made it possible to estimate pelagic primary production, particle export, bottom flux, and subsequent burial of organic carbon with spatial detail. Muller-Karger et al.⁶ estimated that continental margins may be responsible for >40% of the organic carbon sequestration in the ocean. An even higher estimate of 98% for margins was published by Dunne et al.⁷. The same authors also estimated that 85% of the total burial flux

(0.67 ± 0.45 Pg C yr⁻¹) occurred on continental shelves (shallower than 200 m). The latter, however, is in contradiction to de Haas et al.⁸ suggesting that shelf areas do not accumulate substantial amounts of organic carbon under present day conditions and, only locally, are considerable amounts of organic carbon buried. De Haas et al.⁸ concluded that the role of shelves as sinks for organic carbon is overestimated. More recently, it has been claimed that the importance of seafloor sediments as places of organic carbon sequestration is somewhat diminished in comparison to vegetated coastal ecosystems (saltmarshes, mangroves, and seagrass meadows), which would account for 47% of the marine organic carbon burial despite covering only 2% of the ocean surface⁹. Vegetated coastal ecosystems have been a focus of research over the last ten to fifteen years under the concept of Blue Carbon¹⁰. As these ecosystems might be able to remove CO₂ from the atmosphere at high rates, store fixed CO₂ as organic carbon over timescales of centuries or longer, and are frequently threatened by human activities, it has been suggested that management, conservation, and restoration of vegetated coastal ecosystems might significantly contribute to greenhouse gas removal from the atmosphere¹¹. Other ecosystems might satisfy the above definition of actionable Blue Carbon, but research gaps currently preclude them from a classification as either actionable or non-actionable. To fill these research gaps, information on organic carbon sequestration/accumulation rates,

¹Geological Survey of Norway, P.O. Box 6315, Torgarden, 7491 Trondheim, Norway. ²Department of Earth Sciences, Geological Institute, ETH Zürich, Sonneggstrasse 5, 8092 Zürich, Switzerland. ³IC3: Centre for ice, Cryosphere, Carbon and Climate, Department of Geosciences, UiT The Arctic University of Norway, 9037 Tromsø, Norway. ✉e-mail: markus.diesing@ngu.no

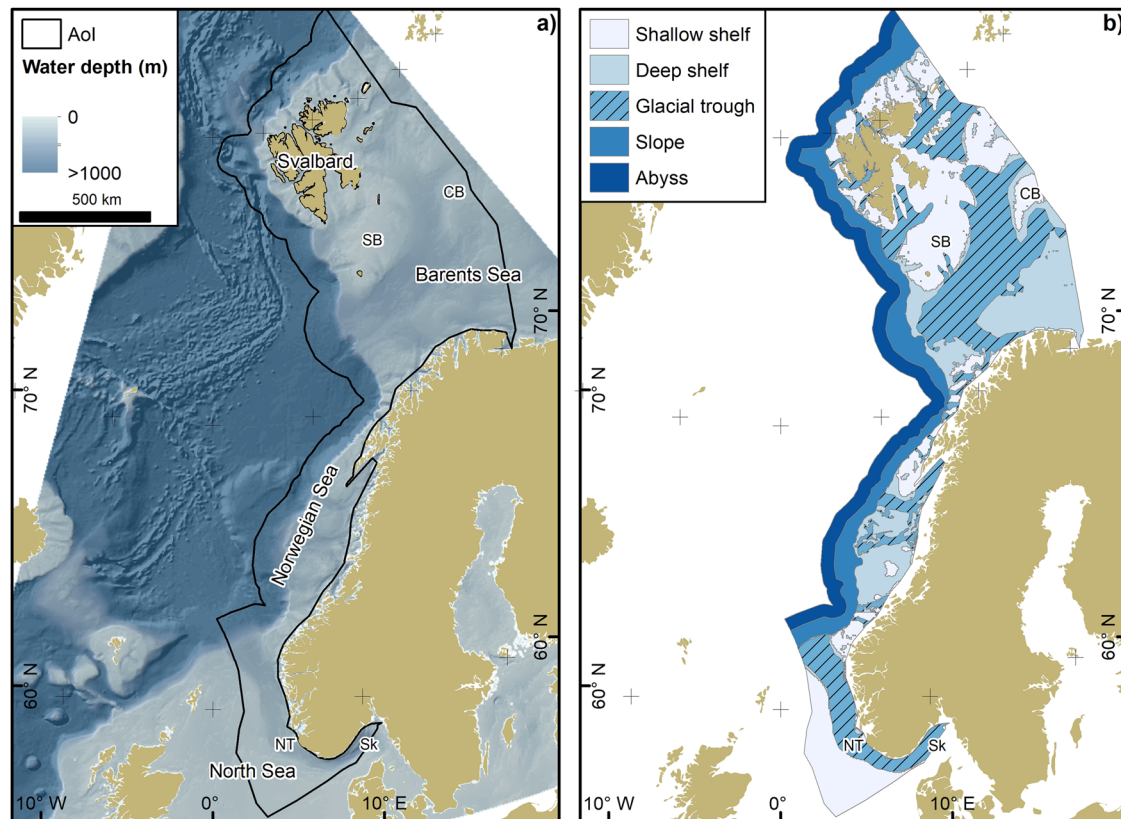


Fig. 1 | Overview of the area of interest (AoI). **a** Water depth⁹⁶, regional seas and locations mentioned in the text. CB Central Bank, NT Norwegian Trough, SB Spitsbergen Bank, Sk Skagerrak. **b** Geomorphological units based on Harris et al.²⁴.

The continental shelf is further subdivided into shallow shelf (0 to 200 m water depth) and deep shelf (200 m depth to the shelf edge).

current organic carbon stocks and their stability, the geographic area, anthropogenic drivers of system loss leading to carbon removals, and emission rates from degraded and intact states is required¹². Emerging Blue Carbon ecosystems include wild and cultivated macroalgae, unvegetated tidal flats, and marine sediments¹³. Continental shelf and slope (margin) sediments might exhibit lower organic carbon stocks and accumulation rates per unit area but cover much larger areas than vegetated coastal ecosystems¹⁴. The large spatial extent might therefore weigh out the lower areal stocks and accumulation rates, but the importance of continental margins as places of organic carbon accumulation and storage relative to vegetated coastal ecosystems is currently not well constrained. While our knowledge on local, regional, and global organic carbon stocks has steeply increased over the past few years^{15–22}, there currently exist knowledge gaps regarding organic carbon accumulation in margin sediments. Specifically, we lack spatially explicit quantifications of organic carbon accumulation rates and related uncertainties in the estimates. Such knowledge gaps could be filled with the application of machine learning spatial models, as exemplified by Diesing et al.¹⁸. Accounting for the complex nature of continental margins with zones of rapid carbon cycling and accumulation juxtaposed^{8,18} will be an important consideration. This study investigates the significance of sediments in terms of organic carbon accumulation and storage potential on the Norwegian continental margin (Fig. 1). We do not aim to estimate organic carbon burial, defined as the balance between the accumulation of organic carbon and its post-depositional degradation, as the reference depths below which organic carbon is assumed to be removed from the short-term surface carbon cycle vary between studies and organic carbon might not even be irreversibly buried or preserved²³. Instead, we estimate the amount of organic carbon that accumulates in the seabed on a timescale of approximately 100–150 years. Our area of interest is the Norwegian continental margin, which spans 26° of latitude and approximately 3000 km between the North Sea and the Arctic Ocean north off Svalbard (Fig. 1). The

formerly glaciated Norwegian continental margin is characterised by a deep shelf break and a continental shelf that is frequently incised by glacial troughs, which are characterised by depths of over 100 m and an over-deepened longitudinal profile that reaches a maximum depth inboard of the shelf break²⁴. We use machine-learning methods to make spatial predictions of dry bulk density, organic carbon content and sediment accumulation rates and quantify the uncertainty in these predictions. In addition, we also estimate the area of applicability, i.e., the area to which a prediction model can be reliably applied²⁵. Based on the spatially predicted properties, we estimate organic carbon accumulation rates and stocks, and provide information on their geographic distribution on the Norwegian continental margin. We show that organic carbon accumulation is spatially highly variable with glacial troughs accounting for nearly half of the total accumulation. The main hotspot of organic carbon accumulation is located in the southernmost part of the study area, the Skagerrak.

Results and discussion

Spatially predicted variables

The characteristics and performance indicators of the three spatial models (dry bulk density, organic carbon content and sediment accumulation rate) are summarised in Table 1. The performance indicators mean error (which measures bias), r-squared (which measures the explained variance) and root mean squared error (which measures accuracy) were derived in a spatial cross-validation scheme. Note that there were approximately three times more observations of dry bulk density and organic carbon content than of sediment accumulation rates.

The dry bulk density model was based on 606 observations. It had a mean error of 0.023 g cm⁻³, a root mean squared error of 0.193 g cm⁻³, an explained variance of 70% and an area of applicability²⁵ equal to 93% of the total area (Table 1). Of the 45 predictors initially used for model building, five were selected for the final model. These were, in decreasing order of

Table 1 | Summary of the three models and their performance

| Response variable | Unit | N_{resp} | N_{pred} | ME | RMSE | R^2 | AOA |
|----------------------------|---------------------|-------------------|-------------------|-------|-------|-------|-------|
| Dry bulk density | g cm^{-3} | 606 | 5 | 0.023 | 0.193 | 0.702 | 92.65 |
| Organic carbon content | weight-% | 697 | 11 | 0.019 | 0.239 | 0.822 | 91.68 |
| Sediment accumulation rate | cm yr^{-1} | 220 | 5 | 0.024 | 0.114 | 0.533 | 97.62 |

N_{resp} Number of observations in the response data, N_{pred} Number of the selected predictor variables, ME Mean Error, RMSE Root Mean Squared Error, R^2 explained variance, AOA Area of Applicability as percent of the total area.

importance, predicted probability of substrate class mud, predicted probability of the substrate class sandy mud, distance to land, mean water temperature at the seafloor and predicted probability of the substrate class coarse sediment (Fig. S1). The importance of substrate class for predicting dry bulk density seems intuitive, as dry bulk density is closely related to sediment grain size²⁶.

The organic carbon model was based on 697 observations. It had a mean error of 0.019 weight-%, a root mean squared error of 0.239 weight-%, an explained variance of 82% and an area of applicability²⁵ equal to 92% of the total area (Table 1). Of the 38 predictors initially used for model building, eleven were selected for the final model. The five most important predictors were, in decreasing order of importance, mud content of surficial seafloor sediment, mean primary productivity at the sea surface, bathymetry, mean dissolved molecular oxygen at the seafloor and mean water temperature at the seafloor (Fig. S1). In agreement with previous studies^{19,20,27}, mud content is the most important predictor for organic carbon content. Relationships between fine-grained sediments and organic carbon content have been recognised for a long time²⁸. The observed increases in organic carbon content with increases in mud content have been attributed to sorption of organic matter to mineral surfaces^{29,30}: Surface area increases with decreasing grain size and organic carbon content tends to increase with surface area; hence, fine-grained sediments are associated with higher organic carbon contents. Additionally, diffusion-dominated permeable sediments on the inner shelf might act as biocatalytic filters that effectively remineralise organic matter³¹. Consequently, such mud-free sands exhibit very low organic carbon contents.

The sediment accumulation model was based on 220 observations. It had a mean error of 0.024 cm yr^{-1} , a root mean squared error of 0.114 cm yr^{-1} , an explained variance of 53% and an area of applicability²⁵ equal to 98% of the total area (Table 1). Of the 41 predictors initially used for model building, five were selected for the final model. These were, in decreasing order of importance, mud content of surficial seafloor sediment, minimum surface swept area ratio (fishing intensity), relative probability of predicted sedimentary environment 'no or very slow deposition', and maximum and range of partial pressure of CO_2 at the sea surface (Fig. S1). Mud content has been identified as the most important predictor. This might indicate correlation rather than causation, as both sediment accumulation rates and mud content tend to be higher in hydrodynamically quiet environments and vice versa.

All three models have a low mean error close to zero, indicating that they are nearly unbiased. The explained variance of the organic carbon model is comparable to studies which did not employ spatial cross-validation^{19,22}. The explained variance of the sediment accumulation model is comparable to other regional studies, which reported an explained variance of 42% for the Baltic Sea³² and 58% for the North Sea and Skagerrak¹⁸ but did not account for spatial autocorrelation. All models are applicable in more than 90% of the area of interest. The resulting maps are shown in Figs. S2 – S4.

Substantial amounts of organic carbon are stored in continental margin sediments

All analyses are restricted to the joint area of applicability of the dry bulk density and organic carbon models, covering an area of $978,736 \text{ km}^2$. Organic carbon stocks of the upper 0.1 m of Norwegian seafloor sediments

range between 0.14 and 3.40 kg m^{-2} , while the uncertainty, measured as the 90% prediction interval (see Methods) varies between 0.23 and 4.22 kg m^{-2} (Fig. 2). Uncertainties tend to increase with increasing predicted stocks. Stocks are lowest ($< 0.5 \text{ kg m}^{-2}$) on the North Sea shelf, shelf banks in the Norwegian Sea, along the shelf edge and lower slope and parts of the southern Barents Sea. Conversely, stocks are highest ($> 2 \text{ kg m}^{-2}$) off the northern and western coasts of Svalbard and in a southwest-northeast oriented band from Spitsbergen Bank to Central Bank. However, the calculated stocks on Spitsbergen Bank lie outside the joint area of applicability of the organic carbon and dry bulk density models and might be unrealistic, as coarse sediments³³ and mobile bedforms³⁴ are widespread on the bank (Figs. S5 and S6). Interestingly, the highest stocks as described above are located north of the marginal ice zone (Fig. 2a). In the seasonally sea ice covered northern area, higher stocks could reflect a highly variable primary production regime with efficient vertical export and less recycling than in the southern Barents Sea. Indeed, measured accumulation rates of organic carbon here are more than twice as high as in the ice-free southern region³⁵ reflecting the modern ecosystem³⁶ with higher primary productivity but lower vertical organic flux rates in the southern than in the northern Barents Sea. In addition, sea-ice induced lateral transport and subsequent release of terrestrial organic carbon can further accelerate deposition of primary produced organic carbon in the marginal ice zone³⁷. Glacial troughs tend to have higher organic carbon stocks than their surrounding areas. This contrast is particularly stark between the Norwegian Trough and the North Sea shelf, indicating that shelf sediments can act in distinctly different ways in the context of organic carbon processing¹⁸. Indeed, centres of organic carbon accumulation and oxidation³⁸ might lie in close proximity to each other.

The mean organic carbon stock in margin sediments off Norway is $0.83 \pm 0.47 \text{ kg m}^{-2}$. Mean organic carbon stocks vary across geomorphological units (Fig. 3a). They are highest in glacial troughs ($1.02 \pm 0.41 \text{ kg m}^{-2}$) and lowest in the abyss ($0.55 \pm 0.17 \text{ kg m}^{-2}$). Statistical tests of the differences of mean organic carbon stocks between geomorphological units using a one-way analysis of variance test show that there is a statistically significant difference in mean organic carbon stocks between at least two geomorphological units ($F(4) = 220.3$, $p < 0.001$). A Tukey post-hoc test for multiple comparisons has found that the mean value of organic carbon stocks is significantly different between all pairs of geomorphological units (adjusted $p < 0.001$, 99% confidence level).

As expected¹⁴, mean organic carbon stocks are lower than those of salt marshes (3.31 kg m^{-2}) and seagrass meadows (2.41 kg m^{-2}) in the Nordic countries (Greenland, Iceland, Faroe Islands, Norway, Denmark, Sweden, and Finland)³⁹. However, this is outweighed by the much larger area occupied by margin sediments ($978,736 \text{ km}^2$) as compared to salt marshes (1440 km^2) and seagrass meadows (1861 km^2)³⁹. The reservoir size of margin sediments in Norway thus amounts to 814 Tg C (90% prediction interval: 1203 Tg C), and thereof 320 Tg C (39%) is stored in glacial troughs (Fig. 3b). For comparison, current best estimates of reservoir sizes in vegetated coastal ecosystems in the Nordic countries amount to 4.47 Tg C for salt marshes and 4.49 Tg C for seagrass meadows³⁹. However, Krause-Jensen et al.³⁹ consider these estimates as preliminary and in need of further validation. Despite the remaining uncertainties in the estimates, continental margin sediments constitute a substantial store of organic carbon that has so far been overlooked.

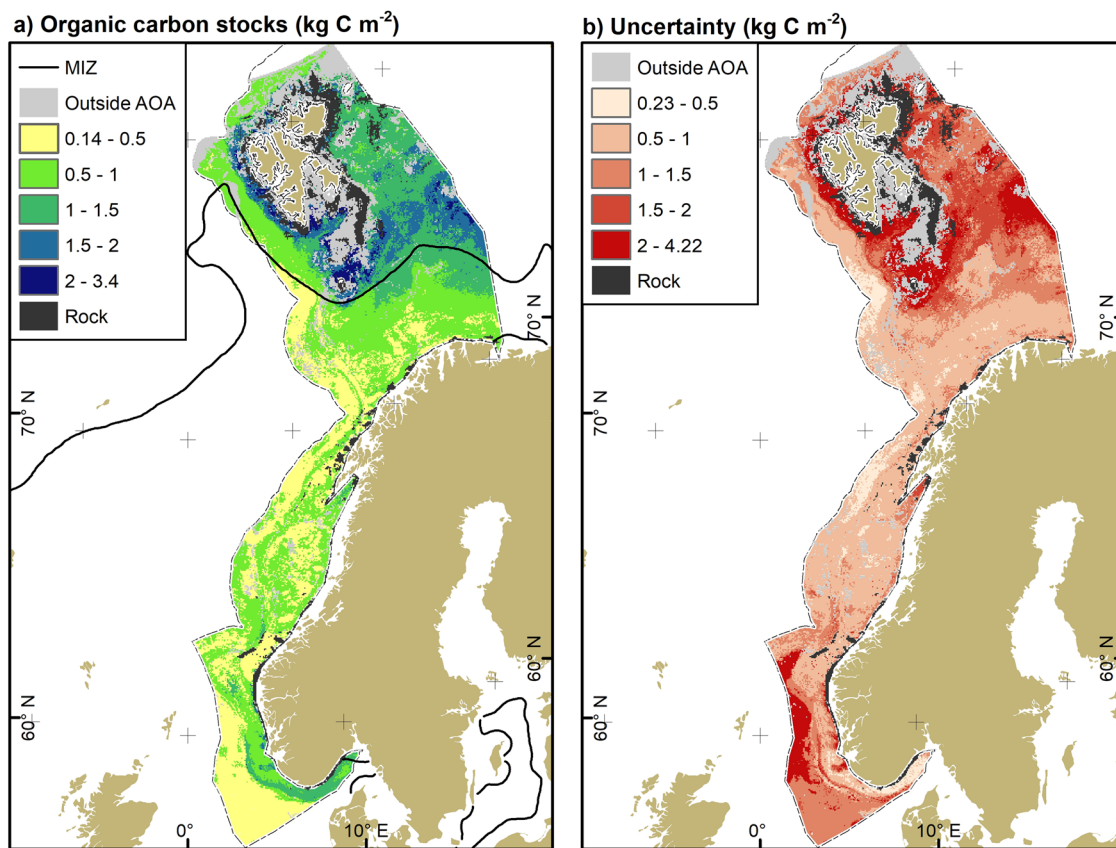


Fig. 2 | Organic carbon stocks of surficial (0–10 cm) sediments on the Norwegian continental margin. Stocks have been calculated from predicted dry bulk densities (Fig. S2) and organic carbon contents (Fig. S3). **a** Estimated organic carbon stocks (kg C m^{-2}). MIZ marginal ice zone based on Itkin et al.⁹⁷. **b** Prediction uncertainty

(kg C m^{-2}), expressed as the 90% prediction interval. Areas outside the joint area of applicability (AOA) are shown in grey. Areas predicted as rock in the substrate type model (Fig. S5) have been excluded from the analysis.

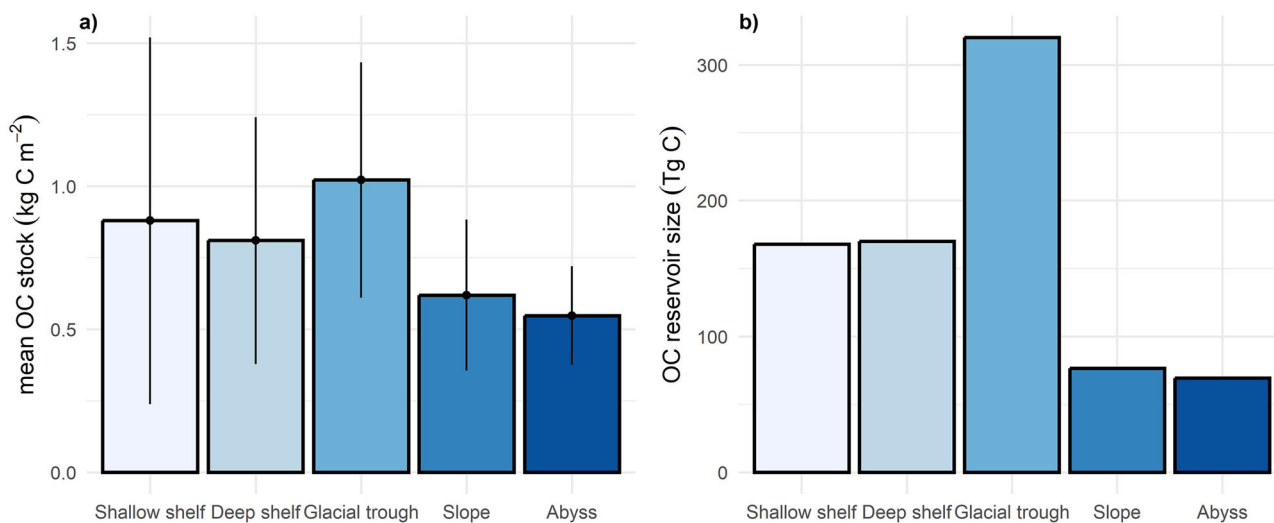


Fig. 3 | Organic carbon (OC) stocks (0–10 cm) of the geomorphological units as shown in Fig. 1. **a** Mean organic carbon stocks averaged over the five morphological units. Vertical lines indicate one standard deviation. **b** Organic carbon reservoir sizes.

Complex patterns of organic carbon accumulation

As we used ²¹⁰Pb-derived sediment accumulation rates, the following estimates refer to accumulation over the last 100–150 yr based on its half-life of 22.2 yr and an integration time of approximately five to seven times the half-life⁴⁰.

All analyses are restricted to the joint area of applicability of the dry bulk density, organic carbon, and sediment accumulation rate models,

covering an area of 961,664 km². Organic carbon accumulation rates range from 0.0 to 123.1 $\text{g C m}^{-2} \text{yr}^{-1}$, with uncertainties varying between 4.5 and 284.8 $\text{g C m}^{-2} \text{yr}^{-1}$ (Fig. 4a and b). Uncertainties tend to increase with increases in the predicted accumulation rates. Zero-accumulation of organic carbon (yellow areas in Fig. 4a) is linked to the North Sea shelf, the shelf break, shelf banks in the Norwegian Sea, and Spitsbergen Bank, the latter in agreement with Pathirana et al.⁴¹. The main hotspot of organic carbon

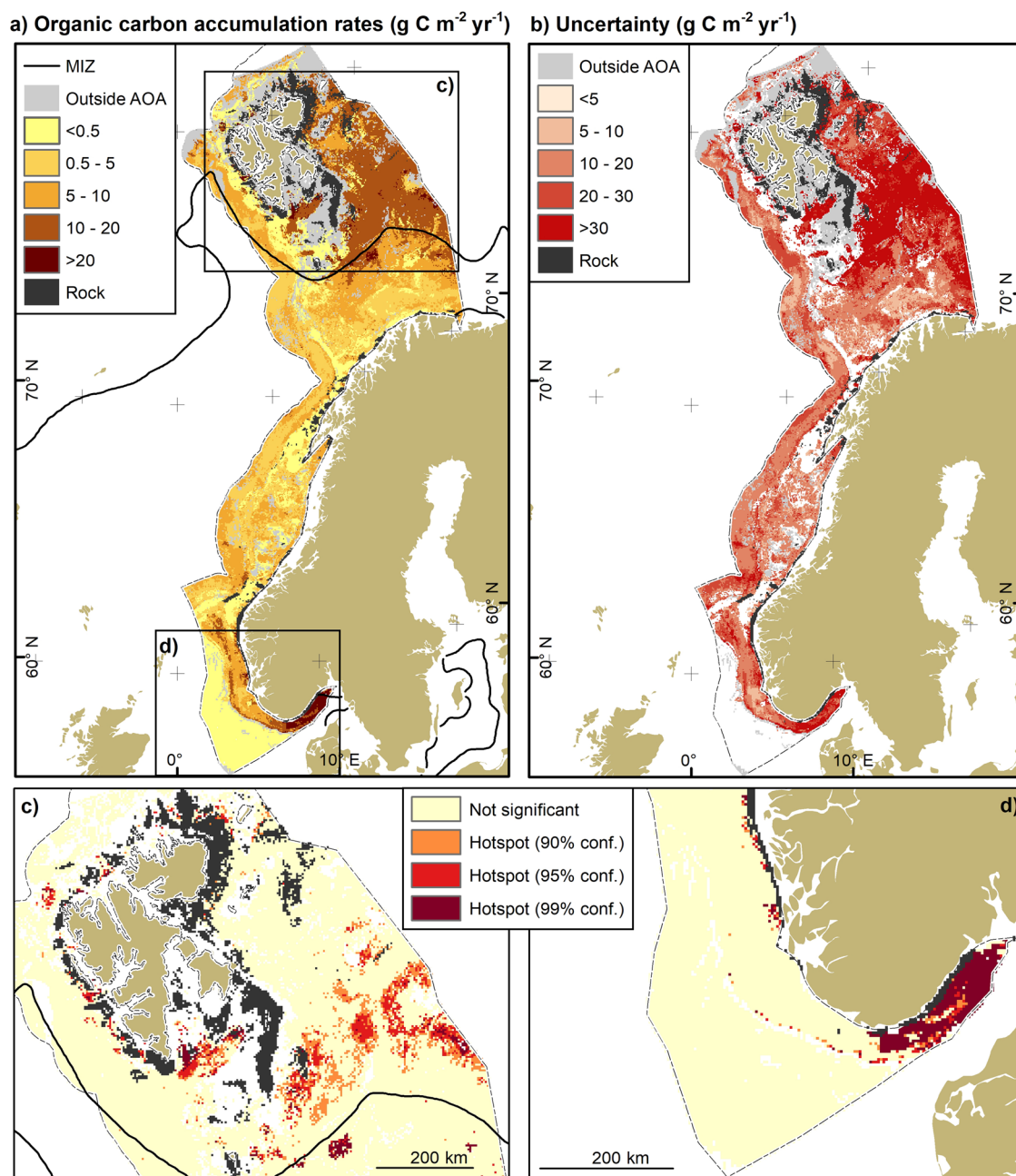


Fig. 4 | Organic carbon accumulation rates on the Norwegian continental margin. Organic carbon accumulation rates were calculated from organic carbon stocks of surficial (0–10 cm) sediments (Fig. 2) and sediment accumulation rates (Fig. S4). **a** Estimated organic carbon accumulation rates ($\text{g C m}^{-2} \text{yr}^{-1}$). MIZ – marginal ice zone based on Itkin et al.⁹⁷. **b** Prediction uncertainty ($\text{g C m}^{-2} \text{yr}^{-1}$), expressed as the 90% prediction interval. Note that the uncertainty is not defined in areas with

sedimentation rates of 0 cm yr^{-1} (see Eq. 7). Areas outside the joint area of applicability (AOA) are shown in grey. Areas predicted as rock in the substrate type model (Fig. S5) were excluded from the analysis. **c** Statistically significant hotspots of organic carbon accumulation in the Barents Sea at three levels of confidence. **d** Same as (c) for the North Sea and Skagerrak.

accumulation in terms of size and confidence is to be found in the inner part of the Norwegian Trough in the Skagerrak (Fig. 4d). Additionally, hotspots are widespread in the Barents Sea mainly north of the marginal ice zone. However, these are less contiguous, smaller in size and lower in confidence (Fig. 4c). No hotspots of noticeable size are located in the Norwegian Sea. Geomorphology acts as a driver of the patterns of organic carbon accumulation (Fig. 5a): Mean rates are lowest on the continental slope ($3.88 \pm 2.69 \text{ g C m}^{-2} \text{yr}^{-1}$) and shallow continental shelf ($4.23 \pm 6.42 \text{ g C m}^{-2} \text{yr}^{-1}$), and highest in glacial troughs ($9.29 \pm 6.89 \text{ g C m}^{-2} \text{yr}^{-1}$), where they are more than twice as high. Intermediate mean rates are to be found on the deep continental shelf ($5.48 \pm 5.03 \text{ g C m}^{-2} \text{yr}^{-1}$) and the abyss ($5.26 \pm 2.18 \text{ g C m}^{-2} \text{yr}^{-1}$). We have tested the statistical significance of the

differences of mean organic carbon accumulation rates between geomorphological units. There is a statistically significant difference in mean organic carbon accumulation rates between at least two geomorphological units based on a one-way analysis of variance test ($F(4) = 181.5, p < 0.001$). A Tukey post-hoc test for multiple comparisons has found that the mean value of organic carbon accumulation rates is significantly different between all pairs of geomorphological units (adjusted $p < 0.001$, 99% confidence level), except for the combinations shallow shelf–abyss (adjusted $p < 0.005$), deep shelf – abyss and slope – shallow shelf (both adjusted $p > 0.1$).

Nearly half (48%) of the accumulation of organic carbon is happening in glacial troughs (Fig. 5b) due to their high accumulation rates per unit area (Fig. 5a) and the large areas they occupy on the Norwegian continental

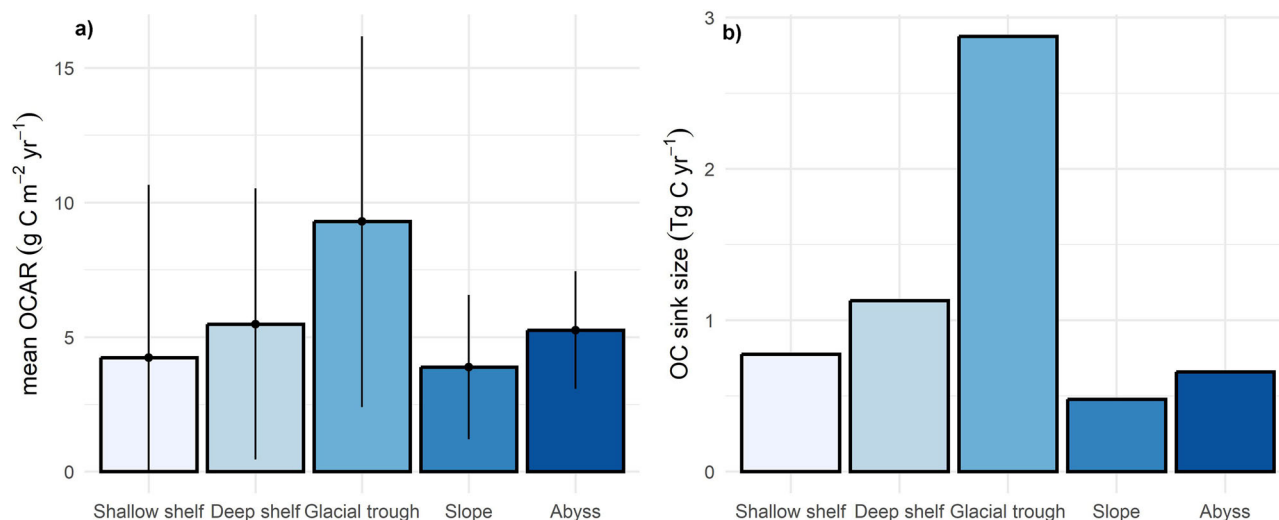


Fig. 5 | Organic carbon accumulation rates (OCAR) of the geomorphological units as shown in Fig. 1. a Mean organic carbon accumulation rates averaged over the five morphological units. Vertical lines indicate one standard deviation. **b** Organic carbon sink sizes.

margin (Fig. 1), amounting to 346,520 km². Glacial troughs are therefore centres of organic carbon accumulation on the Norwegian continental margin. They are seaward continuations of fjord systems, which have been associated with high rates of organic carbon accumulation⁴².

Aggregated over the joint area of applicability, the sediments of the Norwegian continental margin accumulate 6.0 Tg C yr⁻¹ (90% prediction interval: 18.7 Tg C yr⁻¹). For comparison, salt marshes and seagrass meadows might accumulate 0.20 and 0.021 Tg C yr⁻¹ in the Nordic countries, respectively³⁹. As for organic carbon stocks, the latter estimates are very coarse and preliminary³⁹. Expressed in equivalents of CO₂, Norwegian margin sediments accumulate 22 Tg CO₂-eq per year within the joint area of applicability. This is equivalent to 45% of Norway's greenhouse gas emissions of 48.9 Tg CO₂-eq in 2022⁴³.

The most extensive vegetated coastal ecosystems in Norway are macroalgae. Intertidal and subtidal rockweed and subtidal kelp cover 3090 km² and 7417 km², respectively^{39,44}. As most macroalgae attach to hard substrates, they do not store organic carbon in sediments beneath the vegetation. However, macroalgae export part of their photosynthetic production as particulate and dissolved organic carbon to other habitats including continental shelf and deep-sea sediments⁴⁵. Few studies have so far attempted to quantify these processes. A first tentative estimate^{39,44} of macroalgae particulate organic carbon sequestration rates of 19.9 g C m⁻² yr⁻¹ (based on a mass balance approach comparable to ref. 45) allows us to calculate a potential subsidy of 0.21 Tg C yr⁻¹ of particulate organic carbon from macroalgae to the estimated 6.0 Tg C yr⁻¹ in Norwegian margin sediments. Roughly 3.5% of the organic carbon accumulating in margin sediments might thus derive from macroalgae.

Climate mitigation potential of margin sediments

Vegetated coastal ecosystems (mangroves, saltmarshes, and seagrass meadows) have been framed as a natural climate solution⁴⁶. However, recent studies have cast some doubt on the role of vegetated coastal ecosystems in the context of climate mitigation: (1) Existing organic carbon stocks are rather a liability than an asset⁴⁷. (2) The magnitude of the effect is too small^{47,48}. (3) There is a timescale mismatch between ancient fossil fuel emissions and uptake by vegetation⁴⁷. We discuss to what extent these issues might also affect organic carbon in margin sediments.

Stocks as a liability. Organic carbon stocks (measured in kg C m⁻² within a certain sediment depth interval) and the associated reservoir sizes (Tg C) are basic metrics and so far, most marine studies^{16,17,19,21} have only quantified these. Organic carbon stored in surficial marine sediments is indeed prone to disturbance by human activities such as

demersal fisheries⁴⁹, seafloor cabling⁵⁰, wind farm installations⁵¹, and deep-sea mining⁵². Providing estimates of organic carbon stocks is hence crucial considering the expansion of the mentioned anthropogenic activities. Our study provides relevant information on the spatial distribution of surficial organic carbon stocks on the Norwegian continental margin (Fig. 2). Together with spatial data on fishing activity, these data could be used to identify priority areas to manage mobile bottom fishing⁵³. Areas with high organic carbon stocks might be considered for protection from disturbance by mobile bottom fishing⁵⁴ with the aim to reduce the release of CO₂ into the water column and potentially the atmosphere⁵⁵. In that sense, we agree that organic carbon stocks of continental margin sediments are a potential liability, but it is vital to map them with the aim to improve our understanding of the impacts of human activities on these stocks and facilitate their management.

Magnitude of the carbon removal effect. Although estimates of organic carbon accumulation in Norwegian salt marshes and seagrass meadows are preliminary, we have shown that margin sediments accumulate considerably more organic carbon because of their much larger extent. The organic carbon accumulation in margin sediments might be subsidised by particulate organic carbon originating from the extensive beds of macroalgae along the Norwegian coast on the order of 3.5%. We therefore conclude that the potential of margin sediments for removing carbon is high when compared with vegetated coastal ecosystems in Norway and should no longer be overlooked.

Further, we have demonstrated that glacial troughs are the main centres of organic carbon accumulation on the Norwegian continental margin, with accumulation rates significantly higher than in other geomorphological units. Globally, glacial troughs are found on the formerly glaciated continental margins of North America, Eurasia, south America, and Antarctica, covering 3.66 million km² of the seabed²⁴. If we assumed that the rate of organic carbon accumulation in glacial troughs of 9.29 ± 6.89 g C m⁻² yr⁻¹ (Fig. 5a) is representative for glacial troughs globally, then these geomorphological features would accumulate 9–59 Tg C yr⁻¹ (based on mean value and standard deviation), which is in the same order of magnitude as fjords (21–25 Tg C yr⁻¹)⁴², seagrass meadows (11.1–27.1 Tg C yr⁻¹)¹³, mangroves (17.5–23.1 Tg C yr⁻¹)⁵⁶, and saltmarshes (8.5 – 9.0 Tg C yr⁻¹)¹³. Although our global estimate (Fig. 6) is currently tentative, it points to a hitherto overlooked environment with high potential for organic carbon accumulation.

These results show that continental margins, and particularly glacial troughs, accumulate organic carbon at scales comparable to or larger than vegetated coastal ecosystems in Norway and potentially globally. To

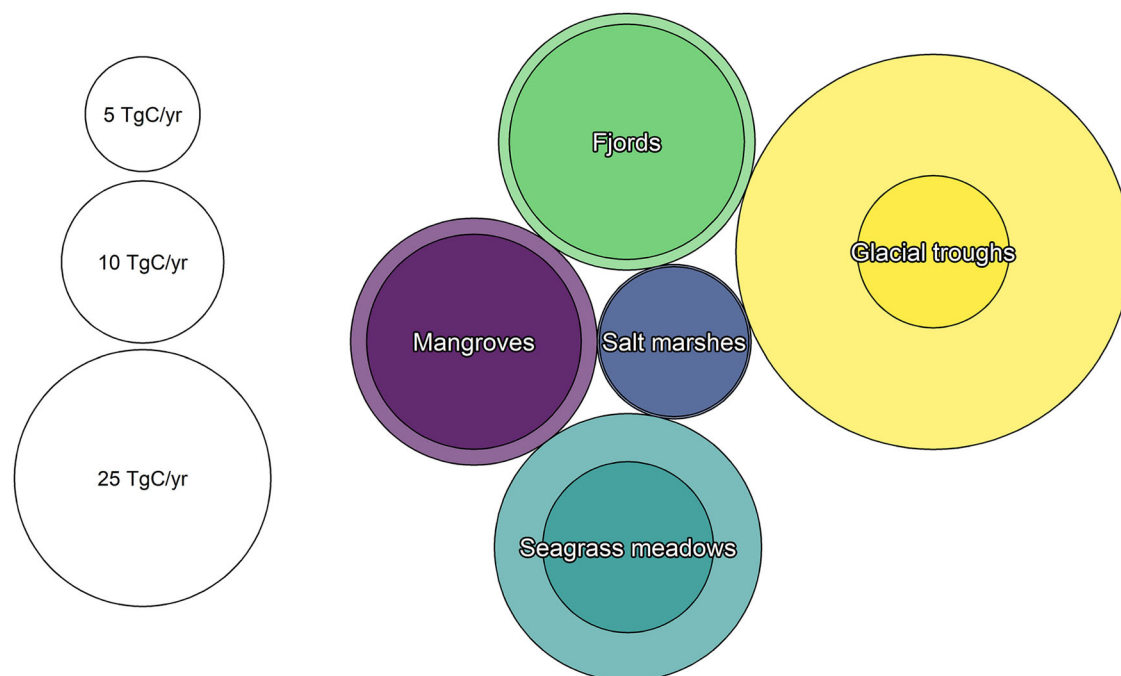


Fig. 6 | Comparison of global organic carbon accumulation potential of vegetated coastal ecosystems^{13,56}, fjords⁴², and glacial troughs (this study). Low and high estimates are indicated by different circle sizes.

perform a climate mitigation service requires, however, increases in carbon removal through management interventions, the so-called additionality. Conceptually, organic carbon accumulation rates are the balance between the incoming flux of organic carbon to the seafloor and the rate of mineralisation of organic carbon at or near the sediment surface⁵⁷. Organic carbon accumulation, and hence carbon removal, could thus be increased by increasing the flux to the seafloor or decreasing the remineralisation rate. Carbon dioxide removal technologies that could increase the incoming flux of carbon to the seafloor such as iron fertilisation⁵⁸, artificial upwelling⁵⁹ and sinking of biomass⁶⁰ have been proposed. For example, a global study found that Norway has the largest area suitable for macroalgae offshore cultivation and sinking⁶¹. However, such technologies are currently at a concept stage and might be controversial due to unintended side effects⁶². Decreasing remineralisation of organic carbon at the seafloor, e.g., by limiting or minimising the impact of mobile bottom fishing gear on organic carbon in surficial seafloor sediments might be a more viable option, and the efficacy of implementing marine protected areas with trawl bans⁶³, temporal trawl closures⁶⁴ and gear modifications⁶⁵ should be considered. We have mapped patterns and hotspots of organic carbon accumulation on the Norwegian continental margin (Fig. 4). Overlaying this map with spatial data of bottom fishing intensity or other anthropogenic activities that may threaten sedimentary organic carbon could help analyse the potential magnitude of the additional carbon removal effect and inform marine management in Norway. Given the likely link between the fixing of CO₂ by seaweeds in the coastal zone and accumulation of seaweed-derived particulate organic carbon in margin sediments, it has also been suggested to spatially protect both source and sink areas through marine protected areas⁶⁶. Forensic carbon accounting⁶⁷ would be required to establish such links on the Norwegian continental margin.

Analysing organic carbon accumulation on continental margins in the context of anthropogenic disturbance globally would be the next logical step to assess the potential of margin sediments to remove carbon and increase the climate mitigation effect. While progress has been made to map demersal fishing activity globally⁶⁸, we lack global maps of organic carbon accumulation. To derive such maps will require (1) data on organic carbon content, dry bulk density and sediment accumulation rates of sufficient quality and quantity, (2) relevant predictor variables of global coverage and

sufficient resolution, and (3) spatial models that consider the complex nature of continental margins, where centres of organic carbon accumulation and remineralisation might be found juxtaposed^{8,18}.

In summary, there currently is limited data to assess the global size of the carbon removal effect of glacial troughs. Our results and comparisons indicate, however, that glacial troughs might be as important as vegetated coastal ecosystems. Given the scale of the carbon dioxide removal required (100–1000 Pg CO₂ over the 21st century⁶⁹), we should not overlook glacial troughs as an option to contribute to this task.

Timescale mismatch. Johannessen and Christian⁴⁷ claim that there is a timescale mismatch between fossil fuel emissions and uptake of carbon dioxide by vegetation: The burning of fossil fuels has led to a perturbation of the geological long-term carbon cycle, which acts over timescales of millions of years². The released carbon dioxide equilibrates between the various carbon reservoirs of the surface carbon cycle on timescales of a few centuries⁷⁰. Removal from the short-term cycle and transfer to the geological carbon cycle is linked to marine sediments, where organic carbon is buried over geological timescales. Accumulation of organic carbon in vegetated coastal ecosystems does not constitute true burial, as the organic carbon that is stored in the biomass and sediment stays within the short-term surface carbon cycle. It can be released back to the atmosphere as carbon dioxide in the case of disturbances, e.g., through land conversion⁷¹ or climate change⁷². Claims that vegetated coastal ecosystems, which cover < 2% of the ocean surface, contribute close to half of the organic carbon burial⁹ are therefore misleading. However, expanding the area or increasing the efficiency of organic carbon accumulation in vegetated coastal ecosystems could draw down carbon dioxide from the atmosphere in the short term, buying time to implement other climate actions⁴⁷.

Carbon dioxide removed from the atmosphere and stored at time scales of ≥ 100 yr is considered sequestered. Organic carbon stored in surface sediments that undergo active remineralisation or are vulnerable to resuspension cannot be said to be sequestered. Only organic carbon accumulation below the vulnerable surface mixed layer represents sequestration⁷³. Sediment mixing, as reflected by the surface mixed layer, appears to strongly impact organic carbon preservation in margin

sediments⁷⁴. On deep glaciated margins, like in Norway, the thickness of the surface mixed layer is 3.6 cm on average⁷⁴. Based on the predicted sediment accumulation rates (Fig. S4), it would take between 5 and 26 yr for organic carbon to reach depths below the surface mixed layer in the organic carbon accumulation hotspot in the Skagerrak (Fig. 4d). Provided adequate protection from human disturbance, the Skagerrak could offer fast carbon removal from the surface mixed layer and permanent storage at timescales of 100 yr and longer. It thus constitutes a prime area for further research in Norway. Although margin sediments do not solve the issue of a timescale mismatch, they offer a perspective of longer-term carbon sequestration and ultimately burial.

Methods

Study site

Our area of interest (Fig. 1) comprises the Norwegian continental shelf and slope²⁴, which we define here as the Norwegian continental margin. We also include the shallowest parts of the abyss (deep sea) within 50 km distance from the seaward boundary of the slope to make best use of existing data. We further subdivide the continental shelf into shallow shelf (above 200 m water depth), deep shelf (between 200 m water depth and the shelf break) and glacial troughs (irrespective of water depth), as mapped by Harris et al.²⁴.

Response data

To derive organic carbon stocks and accumulation rates it is necessary to spatially predict dry bulk density, organic carbon content, and sediment accumulation rates (also referred to as linear sedimentation rates).

Dry bulk density data were obtained from the PANGAEA database⁷⁵ via a data warehouse query. The downloaded data were restricted to the upper 0.1 m of the sediment column. Furthermore, we used data on mud content from the Mareano chemistry database to calculate porosity (ϕ) according to an empirical equation⁷⁶ and ultimately dry bulk density (ρ_d) according to $\rho_d = (1 - \phi)\rho_s$ with grain density, $\rho_s = 2.65 \text{ g cm}^{-3}$. This led to 3218 observations within the area of interest prior to pre-processing (see below).

Data on organic carbon content and ²¹⁰Pb-derived sediment accumulation rates were obtained from the MOSAIC database⁷⁷. The datasets included data from the Mareano chemistry database among others. Data on organic carbon content were restricted to the upper 0.1 m within the area of interest, leading to 2796 observations prior to pre-processing. The dataset on sediment accumulation rates consisted of 237 observations within the area of interest prior to pre-processing.

Datasets compiled from the literature or obtained from databases are frequently biased. For example, sediment accumulation rates are usually only reported in areas where sediments are deposited, and caution is advised when spatially predicting such data⁷⁸. One strategy to deal with this limitation is to include pseudo-observations⁷⁹; in this case records of 0 cm yr^{-1} sediment accumulation in areas that are erosional in nature. Similar approaches have previously been adopted by Diesing et al.¹⁸ and Mitchell et al.³². We randomly placed pseudo samples within the area predicted as Erosion or Transport (Fig. S6). Additionally, we observed that coarse-grained sediments (muddy sandy gravel, sandy gravel, and gravel) were under-represented in our datasets. We therefore included a limited number ($n < 100$) of stations where these sediments had been observed and randomly assigned a sediment composition adhering to their class definitions⁸⁰. These pseudo-observations were used in the dry bulk density dataset.

Predictor variables

We created a raster stack of predictor variables that we considered potentially relevant for predicting the response variables and that were available with (near) full coverage in the area of interest at a sufficiently high spatial resolution. The resolution that was finally chosen was 4 km, which translates to a map scale of approximately 1: 8,000,000 according to a recommended formula in Hengl⁸¹. The raster stack was projected to the Lambert azimuthal equal area projection.

We included variables on seafloor terrain (bathymetry, topographic position, distance to nearest shoreline), ocean colour (chlorophyll-a, primary production and suspended particulate matter), biogeochemistry (surface partial pressure of CO₂, dissolved molecular oxygen of bottom water), sea ice concentration, bottom fishing intensity (swept area ratio), and oceanography (current speed, temperature, and salinity). Multi-annual statistics (mean, minimum, maximum, and range) were calculated for most predictors (Table 2).

In addition, we created predictor layers on substrate types (Tables S1 and S3, Fig. S5), the depositional environment (Tables S2 and S3, Fig. S6), and silt-clay (mud) content of surface sediments (Table S3, Fig. S7) as these were deemed necessary for our study but did not exist (Supplementary Methods).

Spatial predictions

There are many machine learning algorithms available to spatially predict the response variables dry bulk density, organic carbon content and ²¹⁰Pb-derived sediment accumulation rates. We chose the quantile regression forest (QRF) algorithm⁸² on the grounds that it generally performs well and allows to quantify uncertainty (see below). However, predicting sediment accumulation rates has proven challenging in previous studies³² and our initial QRF model performed less well than the other two models. This has led us to also trial Support Vector Machines⁸³. As this did not improve model performance (Table S4) we continued with QRF.

QRF can be seen as an extension of the random forest (RF) algorithm⁸⁴, which has shown high predictive accuracy in several studies across various research domains^{85–88}. RF is an ensemble technique that grows many trees and aggregates the majority class (classification) or conditional mean (regression) from each tree in a forest to make an ensemble prediction. QRF also returns the whole conditional distribution of the response variable, based on which other measures of central tendency (e.g., median) and of prediction uncertainty can be obtained. Following common practice in the global soil mapping community^{89,90}, we used the 90% prediction interval (PI90) as a measure of spatially explicit uncertainty. PI90 gives the range of values within which the true value is expected to occur nine times out of ten, with a one in 20 probability for each of the two tails⁹⁰. It is defined as

$$PI90 = q_{0.95} - q_{0.05} \quad (1)$$

with $q_{0.95}$ and $q_{0.05}$ being the 0.95 and 0.05 quantiles of the distribution, respectively. We chose the median as a measure of central tendency, as the conditional distributions are most likely non-normal, and the median is not affected by extreme outliers.

Prior to modeling, the predictor raster stack was cropped to the area of interest. Areas mapped as Rock and boulders in the substrate type model (Fig. S5) were excluded from further analysis, as we are only interested in the sedimentary environment. The datasets of the response variables organic carbon content and dry bulk density included information on depth below seabed. These datasets were filtered to only include records between 0 cm and 10 cm depth. The response data including sediment accumulation rate were averaged in those cases where more than one value was falling into a grid cell of the predictor stack. This reduced the number of observations of dry bulk density, organic carbon content and sediment accumulation rate to 606, 697 and 220, respectively.

Although it is prudent to initially select a wide range of predictors, it is generally recommended to limit the number of predictors that are finally used for modelling. This is especially true when the number of records in the response data set is low. Variable selection can be achieved in different ways. Here we chose forward feature (variable) selection as implemented in the package CAST⁹¹. The algorithm first trains models based on all possible combinations of two predictor variables. The best combination is retained and tested for the best performance with a third variable. Additional variables are added until the performance stops improving. The model performance was calculated as R² using a spatial cross-validation scheme (see below).

Table 2 | Summary of predictor variables used for spatial prediction

| Variable | Unit | Statistics | Time period | Source |
|---|------------------------------------|--------------------------------|-------------|---|
| Bathymetry | m | - | - | 96 |
| Topographic position index | m | Focal window sizes 25, 75, 125 | - | Calculated from bathymetry |
| Distance to coastline | m | - | - | Calculated |
| Primary productivity | mg m ⁻² d ⁻¹ | Mean, maximum | 2010 – 2019 | Copernicus-GlobColour (https://doi.org/10.48670/moi-00281) |
| Chlorophyll-a concentration | mg m ⁻³ | Mean, maximum | 2010 – 2019 | Copernicus-GlobColour (https://doi.org/10.48670/moi-00281) |
| Suspended particulate matter | g m ⁻³ | Mean, maximum | 2010 – 2019 | Copernicus-GlobColour (https://doi.org/10.48670/moi-00281) |
| Surface partial pressure of CO ₂ | Pa | Minimum, mean, maximum, range | 2010 - 2019 | PISCES GLOBAL_REANALYSIS_BIO_001_029 (https://doi.org/10.25607/OBP-490) |
| Sea ice concentration | - | Minimum, mean, maximum, range | 2010 - 2019 | GLORYS12V1 (https://doi.org/10.48670/moi-00021) |
| Dissolved molecular oxygen | mol m ⁻³ | Minimum, mean, maximum, range | 2000 - 2014 | Bio-ORACLE v2.2 (https://www.bio-oracle.org/index.php) |
| Surface swept area ratio | - | Minimum, mean, maximum, range | 2009 - 2016 | OSPAR (https://odims.ospar.org/en/search/?dataset=bottom_f_intensur) |
| Bottom current speed | m s ⁻¹ | Mean, maximum | 2005 - 2007 | Nordic4k (http://hdl.handle.net/11250/113861) |
| Bottom temperature | °C | Minimum, mean, maximum, range | 2005 - 2007 | Nordic4k (http://hdl.handle.net/11250/113861) |
| Bottom salinity | PSU | Minimum, mean, maximum, range | 2005 - 2007 | Nordic4k (http://hdl.handle.net/11250/113861) |

Model performance needs to be estimated for model tuning, variable selection, and model validation. Model performance estimation is frequently based on k-fold cross validation, whereby the response data are split into k folds, a model is built on k – 1 folds, and validated against the fold which was not used for model building. This process is repeated k times. In standard, non-spatial machine learning applications, this k-fold split is performed randomly on the response data. However, this is not appropriate in the case of spatial data as spatial autocorrelation might lead to inflated estimates of model performance^{92,93}. Folds therefore need to be spatially separated and this was achieved with the k-fold nearest neighbour distance matching algorithm (*knndm* function) of the package CAST⁹⁴.

The performance of the final regression models (dry bulk density, organic carbon content and sediment accumulation rate) was assessed based on the mean error (ME), the explained variance (R²) and the root mean square error (RMSE).

Although it is technically possible to predict the response variable over the full extent of the predictor variables, such predictions might be unreliable where they extrapolate beyond the predictor variable space that has been captured by the model^{25,95}. It has therefore been suggested to estimate the area of applicability (AOA) of a model, where the combination of predictor variables is similar to what the model has been trained with. This can be achieved with the *aoa* function of the package CAST⁹⁴.

Additionally, we used expert judgement to evaluate whether the predicted patterns were reasonable by comparing them with existing maps and a general understanding of the involved processes and their products. Although such an assessment is qualitative and somewhat subjective, it is currently the only way to incorporate expert knowledge and we consider it an essential part of the mapping process.

Calculation of organic carbon stocks

Organic carbon stocks (OCS) are calculated by multiplying the predicted organic carbon contents (*G*) with the predicted dry bulk densities (ρ_d) and the sediment thickness (*d* = 0.1 m):

$$OCS (kg m^{-2}) = \frac{G (\%)}{100} \cdot 1000 \cdot \rho_d (g cm^{-3}) \cdot d (m) \quad (2)$$

Calculations were limited to the joint AOA of the organic carbon and dry bulk density models.

The total reservoir size *m*_{OC} was calculated by summing OCS of all pixels and multiplying with the area of one pixel (*A* = 16,000,000 m²):

$$m_{OC} (Tg) = \left(A (m^2) \cdot \sum OCS (kg m^{-2}) \right) / 1,000,000,000 \quad (3)$$

Calculation of organic carbon accumulation rates

Organic carbon accumulation rates (OCAR) are calculated by multiplying organic carbon contents (0–10 cm) with dry bulk densities and sediment accumulation rates (ω):

$$OCAR (g m^{-2} yr^{-1}) = \frac{G (\%)}{100} \cdot \rho_d (g cm^{-3}) \cdot \omega (cm yr^{-1}) \cdot 10,000 \quad (4)$$

Calculations were limited to the joint AOA of the organic carbon, dry bulk density and sediment accumulation rate models.

The total mass of organic carbon that is accumulated annually (OCA) is calculated by summing OCAR of all pixels and multiplying with the area of one pixel (*A* = 16,000,000 m²):

$$OCA (Tg yr^{-1}) = \left(A (m^2) \cdot \sum OCAR (g m^{-2} yr^{-1}) \right) / 1,000,000,000,000 \quad (5)$$

Propagation of uncertainties

Uncertainties were propagated by taking the square root of the sum of squared relative uncertainties:

$$\delta OCS = OCS \cdot \sqrt{\left(\frac{\delta G}{G}\right)^2 + \left(\frac{\delta \rho_d}{\rho_d}\right)^2} \quad (6)$$

$$\delta OCAR = OCAR \cdot \sqrt{\left(\frac{\delta G}{G}\right)^2 + \left(\frac{\delta \rho_d}{\rho_d}\right)^2 + \left(\frac{\delta \omega}{\omega}\right)^2} \quad (7)$$

The symbol δ signifies the uncertainty of a quantity.

A joint AOA of two or more models was calculated by multiplying the individual AOAs, which had values of 1 (inside AOA) or 0 (outside AOA).

Hotspot analysis

Hotspots of organic carbon accumulation were identified with the Hot Spot Analysis (Getis-Ord G_i^*) tool in ArcGIS 10.8.2, which identifies statistically significant spatial clusters of high values. The calculated organic carbon accumulation rates were converted from raster to point feature format prior to the analysis. Inverse distance was used for the conceptualisation of the spatial relationships and distances were measured as Euclidean distance. The resulting point feature class was converted to a raster file.

Statistical significance testing

We performed statistical tests to analyse the difference between mean organic carbon stocks and accumulation rates of five geomorphological units (Fig. 1). We used a one-way analysis of variance (ANOVA) test to establish whether there is a difference in mean stocks and accumulation rates between geomorphological units. We further performed Tukey's Honestly Significant Difference (HSD) post-hoc test to establish which differences between pairs of geomorphological units are statistically significant. All tests were performed on a stratified random sample ($n = 5000$) drawn from the predicted organic carbon accumulation rates with geomorphological units used as strata. The number of samples was equal for all strata.

Data availability

Calculated organic carbon stocks and accumulation rates and the related uncertainties and areas of applicability are available from PANGAEA: <https://doi.org/10.1594/PANGAEA.965617>. Input (response and predictor variables) and output data of the six spatial models are available at Zenodo: Substrate type: <https://doi.org/10.5281/zenodo.10040165> (input), <https://doi.org/10.5281/zenodo.10053285> (output) Depositional environment: <https://doi.org/10.5281/zenodo.10040720> (input), <https://doi.org/10.5281/zenodo.10053457> (output) Mud content: <https://doi.org/10.5281/zenodo.10057143> (input), <https://doi.org/10.5281/zenodo.10057207> (output) Dry bulk density: <https://doi.org/10.5281/zenodo.10057726> (input), <https://doi.org/10.5281/zenodo.10057750> (output) Organic carbon content: <https://doi.org/10.5281/zenodo.10058434> (input), <https://doi.org/10.5281/zenodo.10058520> (output) Sediment accumulation rates: <https://doi.org/10.5281/zenodo.10061180> (input), <https://doi.org/10.5281/zenodo.10062619> (output) Source data underlying Figs. 1–6 are available from Zenodo: <https://doi.org/10.5281/zenodo.11108526>.

Code availability

The R codes developed to spatially predict the response variables are available at GitHub. Substrate type: <https://github.com/diesing-ngu/GrainSizeReg>. Depositional environment: <https://github.com/diesing-ngu/SedEnv>. Mud content: <https://github.com/diesing-ngu/GSMgrids>. Dry bulk density: <https://github.com/diesing-ngu/DBD>. Organic carbon content: <https://github.com/diesing-ngu/TOC>. Sediment accumulation rates: <https://github.com/diesing-ngu/SedRates>.

Received: 13 December 2023; Accepted: 6 June 2024;

Published online: 15 June 2024

References

- Keil, R. Anthropogenic Forcing of Carbonate and Organic Carbon Preservation in Marine Sediments. *Ann. Rev. Mar. Sci.* **9**, 151–172 (2017).
- Berner, R. A. The long-term carbon cycle, fossil fuels and atmospheric composition. *Nature* **426**, 323 (2003).
- Gershanovich, D. E., Gorshkova, T. I. & Koniukhov, A. I. Organic matter in recent sediments of continental margins. in *Organic matter in recent and fossil sediments and methods of its investigation* (Nauka, Moscow, 1974).
- Berner, R. A. Burial of organic carbon and pyrite sulfur in the modern ocean: Its geochemical and environmental significance. *Am. J. Sci.* **282**, 451–473 (1982).
- Hedges, J. I. & Keil, R. G. Sedimentary organic matter preservation: an assessment and speculative synthesis. *Mar. Chem.* **49**, 81–115 (1995).
- Muller-Karger, F. E. et al. The importance of continental margins in the global carbon cycle. *Geophys. Res. Lett.* **32**, L01602 (2005).
- Dunne, J. P., Sarmiento, J. L. & Gnanadesikan, A. A synthesis of global particle export from the surface ocean and cycling through the ocean interior and on the seafloor. *Global Biogeochem. Cycles* **21**, GB4006 (2007).
- de Haas, H., van Weering, T. C. E. & de Stigter, H. Organic carbon in shelf seas: sinks or sources, processes and products. *Cont. Shelf Res.* **22**, 691–717 (2002).
- Duarte, C. M., Middelburg, J. J. & Caraco, N. Major role of marine vegetation on the oceanic carbon cycle. *Biogeosciences* **2**, 1–8 (2005).
- Nellemann, C. et al. Blue Carbon. A Rapid Response Assessment. United Nations Environment Programme, GRID-Arendal, 80pp. (2009).
- Lovelock, C. E. & Duarte, C. M. Dimensions of Blue Carbon and emerging perspectives. *Biol. Lett.* **15**, 20180781 (2019).
- Howard, J. et al. Clarifying the role of coastal and marine systems in climate mitigation. *Front Ecol. Environ.* **15**, 42–50 (2017).
- Howard, J. et al. Blue carbon pathways for climate mitigation: Known, emerging and unlikely. *Mar. Policy* **156**, 105788 (2023).
- Graves, C. A. et al. Sedimentary carbon on the continental shelf: Emerging capabilities and research priorities for Blue Carbon. *Front Mar. Sci.* **9**, 926215 (2022).
- Hunt, C. et al. Quantifying Marine Sedimentary Carbon: A New Spatial Analysis Approach Using Seafloor Acoustics, Imagery, and Ground-Truthing Data in Scotland. *Front Mar. Sci.* **7**, 588 (2020).
- Smeaton, C., Hunt, C. A., Turrell, W. R. & Austin, W. E. N. Marine Sedimentary Carbon Stocks of the United Kingdom's Exclusive Economic Zone. *Front Earth Sci. (Lausanne)* **9**, 50 (2021).
- Legge, O. et al. Carbon on the Northwest European Shelf: Contemporary Budget and Future Influences. *Front Mar. Sci.* **7**, 143 (2020).
- Diesing, M., Thorsnes, T. & Bjarnadóttir, L. R. Organic carbon densities and accumulation rates in surface sediments of the North Sea and Skagerrak. *Biogeosciences* **18**, 2139–2160 (2021).
- Diesing, M. et al. Predicting the standing stock of organic carbon in surface sediments of the North–West European continental shelf. *Biogeochemistry* **135**, 183–200 (2017).
- Wilson, R. J., Speirs, D. C., Sabatino, A. & Heath, M. R. A synthetic map of the north-west European Shelf sedimentary environment for applications in marine science. *Earth Syst. Sci. Data* **10**, 109–130 (2018).
- Atwood, T. B., Witt, A., Mayorga, J., Hammill, E. & Sala, E. *Glob. Patterns Mar. Sediment Carbon Stocks Front Mar. Sci.* **7**, 165 (2020).
- Lee, T. R., Wood, W. T. & Phrampus, B. J. A Machine Learning (kNN) Approach to Predicting Global Seafloor Total Organic Carbon. *Glob. Biogeochem. Cycles* **33**, 37–46 (2019).

23. Bradley, J. A., Hülse, D., LaRowe, D. E. & Arndt, S. Transfer efficiency of organic carbon in marine sediments. *Nat. Commun.* **13**, 7297 (2022).
24. Harris, P. T., Macmillan-Lawler, M., Rupp, J. & Baker, E. K. Geomorphology of the oceans. *Mar. Geol.* **352**, 4–24 (2014).
25. Meyer, H. & Pebesma, E. Predicting into unknown space? Estimating the area of applicability of spatial prediction models. *Methods. Ecol. Evol.* **12**, 1620–1633 (2021).
26. Flemming, B. W. & Delafontaine, M. T. Mass physical properties of muddy intertidal sediments: some applications, misapplications and non-applications. *Cont. Shelf Res.* **20**, 1179–1197 (2000).
27. Pace, M. C. et al. Modelling seabed sediment physical properties and organic matter content in the Firth of Clyde. *Earth Syst. Sci. Data* **13**, 5847–5866 (2021).
28. Premuzic, E. T., Benkovitz, C. M., Gaffney, J. S. & Walsh, J. J. The nature and distribution of organic matter in the surface sediments of world oceans and seas. *Org. Geochem.* **4**, 63–77 (1982).
29. Keil, R. G. & Hedges, J. I. Sorption of organic matter to mineral surfaces and the preservation of organic matter in coastal marine sediments. *Chem. Geol.* **107**, 385–388 (1993).
30. Mayer, L. M. Surface area control of organic carbon accumulation in continental shelf sediments. *Geochim Cosmochim. Acta* **58**, 1271–1284 (1994).
31. Huettel, M., Berg, P. & Kostka, J. E. Benthic Exchange and Biogeochemical Cycling in Permeable Sediments. *Ann. Rev. Mar. Sci.* **6**, 23–51 (2014).
32. Mitchell, P. J., Spence, M. A., Aldridge, J., Kotilainen, A. T. & Diesing, M. Sedimentation rates in the Baltic Sea: A machine learning approach. *Cont. Shelf Res.* **214**, 104325 (2021).
33. Bjørlykke, K., Bue, B. & Elverhøi, A. Quaternary sediments in the northwestern part of the Barents Sea and their relation to the underlying Mesozoic bedrock. *Sedimentology* **25**, 227–246 (1978).
34. Bellec, V. K. et al. Sandbanks, sandwaves and megaripples on Spitsbergenbanken, Barents Sea. *Mar. Geol.* **416**, 105998 (2019).
35. Faust, J. C. et al. Does Arctic warming reduce preservation of organic matter in Barents Sea sediments? *Philosophical Transactions of the Royal Society A: Mathematical. Phys. Eng. Sci.* **378**, 20190364 (2020).
36. Reigstad, M., Carroll, J., Slagstad, D., Ellingsen, I. & Wassmann, P. Intra-regional comparison of productivity, carbon flux and ecosystem composition within the northern Barents Sea. *Prog. Oceanogr.* **90**, 33–46 (2011).
37. Knies, J. & Martinez, P. Organic matter sedimentation in the western Barents Sea region: Terrestrial and marine contribution based on isotopic composition and organic nitrogen content. *Nor. J. Geol.* **89**, 79–89 (2009).
38. Bianchi, T. S. et al. Centers of organic carbon burial and oxidation at the land-ocean interface. *Org. Geochem.* **115**, 138–155 (2018).
39. Krause-Jensen, D. et al. Nordic Blue Carbon Ecosystems: Status and Outlook. *Front Mar. Sci.* **9**, 847544 (2022).
40. Goldberg, E. D. Geochronology with Pb-210. in *Radioactive Dating. Proc. of the Symposium on Radioactive Dating Held by the International Atomic Energy Agency in Co-operation with the Joint Commission on Applied Radioactivity*. 121–131 (Athens, 1963).
41. Pathirana, I., Knies, J., Felix, M. & Mann, U. Towards an improved organic carbon budget for the western Barents Sea shelf. *Climate* **10**, 569–587 (2014).
42. Smith, R. W., Bianchi, T. S., Allison, M., Savage, C. & Galy, V. High rates of organic carbon burial in fjord sediments globally. *Nat. Geosci.* **8**, 450–453 (2015).
43. SSB. Emissions to air. <https://www.ssb.no/en/natur-og-miljo/forurensing-og-klima/statistikk/utslipp-til-luft> (2023).
44. Frigstad, H. et al. *Blue Carbon - Climate Adaptation, CO2 Uptake and Sequestration of Carbon in Nordic Blue Forests*. (Nordic Council of Ministers Copenhagen, 2020).
45. Krause-Jensen, D. & Duarte, C. M. Substantial role of macroalgae in marine carbon sequestration. *Nat. Geosci.* **9**, 737–742 (2016).
46. Macreadie, P. I. et al. Blue carbon as a natural climate solution. *Nat. Rev. Earth Environ.* **2**, 826–839 (2021).
47. Johannessen, S. C. & Christian, J. R. Why blue carbon cannot truly offset fossil fuel emissions. *Commun. Earth Environ.* **4**, 411 (2023).
48. Taillardat, P., Friess, D. A. & Lupascu, M. Mangrove blue carbon strategies for climate change mitigation are most effective at the national scale. *Biol. Lett.* **14**, 20180251 (2018).
49. Epstein, G., Middelburg, J. J., Hawkins, J. P., Norris, C. R. & Roberts, C. M. The impact of mobile demersal fishing on carbon storage in seabed sediments. *Glob. Chang Biol.* **00**, 1–20 (2022).
50. Clare, M. A., Lichtschlag, A., Paradis, S. & Barlow, N. L. M. Assessing the impact of the global subsea telecommunications network on sedimentary organic carbon stocks. *Nat. Commun.* **14**, 2080 (2023).
51. De Borger, E. et al. Offshore Windfarm Footprint of Sediment Organic Matter Mineralization Processes. *Front Mar. Sci.* **8**, 632243 (2021).
52. Haffert, L., Haeckel, M., de Stigter, H. & Janssen, F. Assessing the temporal scale of deep-sea mining impacts on sediment biogeochemistry. *Biogeosciences* **17**, 2767–2789 (2020).
53. Epstein, G. & Roberts, C. M. Identifying priority areas to manage mobile bottom fishing on seabed carbon in the UK. *PLOS Clim.* **1**, 1–21 (2022).
54. Jankowska, E., Pelc, R., Alvarez, J., Mehra, M. & Frischmann, C. J. Climate benefits from establishing marine protected areas targeted at blue carbon solutions. *Proc. Natl Acad. Sci.* **119**, e2121705119 (2022).
55. Atwood, T. B. et al. Atmospheric CO2 emissions and ocean acidification from bottom-trawling. *Front Mar. Sci.* **10**, 1125137 (2024).
56. Breithaupt, J. L. & Steinmuller, H. E. Refining the Global Estimate of Mangrove Carbon Burial Rates Using Sedimentary and Geomorphic Settings. *Geophys Res Lett.* **49**, e2022GL100177 (2022).
57. Middelburg, J. J. Carbon Processing at the Seafloor. in *Marine Carbon Biogeochemistry: A Primer for Earth System Scientists* 57–75 (Springer International Publishing, Cham, 2019). https://doi.org/10.1007/978-3-030-10822-9_4.
58. Martin, P. et al. Iron fertilization enhanced net community production but not downward particle flux during the Southern Ocean iron fertilization experiment LOHAFEX. *Glob. Biogeochem. Cycles* **27**, 871–881 (2013).
59. Jürchott, M., Oschlies, A. & Koeve, W. Artificial Upwelling—A Refined Narrative. *Geophys. Res. Lett.* **50**, e2022GL101870 (2023).
60. Raven, M. R. et al. Biomass Storage in Anoxic Marine Basins: Initial Estimates of Geochemical Impacts and CO2 Sequestration Capacity. *AGU Adv.* **5**, e2023AV000950 (2024).
61. Alevizos, E. & Barillé, L. Global ocean spatial suitability for macroalgae offshore cultivation and sinking. *Front. Mar. Sci.* **10**, 1320642 (2023).
62. Chopin, T. et al. Deep-ocean seaweed dumping for carbon sequestration: Questionable, risky, and not the best use of valuable biomass. *One Earth* <https://doi.org/10.1016/j.oneear.2024.01.013> (2024).
63. Roberts, C. M. et al. Marine reserves can mitigate and promote adaptation to climate change. *Proc. Natl Acad. Sci.* **114**, 6167 LP–6166175 (2017).
64. Paradis, S. et al. Persistence of Biogeochemical Alterations of Deep-Sea Sediments by Bottom Trawling. *Geophys. Res. Lett.* **48**, e2020GL091279 (2021).
65. Tiano, J. C. et al. Acute impacts of bottom trawl gears on benthic metabolism and nutrient cycling. *ICES J. Mar. Sci.* **76**, 1917–1930 (2019).
66. Queirós, A. M. et al. Identifying and protecting macroalgae detritus sinks toward climate change mitigation. *Ecol. Appl.* **33**, e2798 (2023).
67. Hurd, C. L. et al. Forensic carbon accounting: Assessing the role of seaweeds for carbon sequestration. *J. Phycol.* **58**, 347–363 (2022).

68. Kroodsma, D. A. et al. Tracking the global footprint of fisheries. *Science* (1979) **359**, 904–908 (2018).
69. IPCC. Summary for Policymakers. Global Warming of 1.5°C. An IPCC Special Report on the Impacts of Global Warming of 1.5°C above Pre-Industrial Levels. Global Warming of 1.5°C. An IPCC Special Report on the impacts of global warming of 1.5°C above pre-industrial levels and related global greenhouse gas emission pathways, in the context of strengthening the global response to the threat of climate change, (2018).
70. Archer, D. et al. Atmospheric Lifetime of Fossil Fuel Carbon Dioxide. *Annu Rev. Earth Planet Sci.* **37**, 117–134 (2009).
71. Pendleton, L. et al. Estimating Global “Blue Carbon” Emissions from Conversion and Degradation of Vegetated Coastal Ecosystems. *PLoS One* **7**, e43542 (2012).
72. Barksdale, M. B., Hein, C. J. & Kirwan, M. L. Shoreface erosion counters blue carbon accumulation in transgressive barrier-island systems. *Nat. Commun.* **14**, 8425 (2023).
73. Johannessen, S. C. How can blue carbon burial in seagrass meadows increase long-term, net sequestration of carbon? A critical review. *Environ. Res. Lett.* **17**, 93004 (2022).
74. Song, S. et al. A global assessment of the mixed layer in coastal sediments and implications for carbon storage. *Nat. Commun.* **13**, 4903 (2022).
75. Felden, J. et al. PANGAEA - Data Publisher for Earth & Environmental Science. *Sci. Data* **10**, 347 (2023).
76. Jenkins, C. Summary of the onCALCULATION methods used in dbSEABED. <http://pubs.usgs.gov/ds/2006/146/docs/onCALCULATION.pdf> (2005).
77. Paradis, S. et al. The Modern Ocean Sediment Archive and Inventory of Carbon (MOSAIC): version 2.0. *Earth Syst. Sci. Data* **15**, 4105–4125 (2023).
78. Jenkins, C. Sediment Accumulation Rates For the Mississippi Delta Region: a Time-interval Synthesis. *J. Sediment. Res.* **88**, 301–309 (2018).
79. Hengl, T. et al. SoilGrids250m: Global gridded soil information based on machine learning. *PLoS One* **12**, 1–40 (2017).
80. Folk, R. L. The distinction between grain size and mineral composition in sedimentary-rock nomenclature. *J. Geol.* **62**, 344–359 (1954).
81. Hengl, T. Finding the right pixel size. *Comput Geosci.* **32**, 1283–1298 (2006).
82. Meinshausen, N. Quantile Regression Forests. *J. Mach. Learn. Res.* **7**, 983–999 (2006).
83. Cortes, C. & Vapnik, V. Support-vector networks. *Mach. Learn* **20**, 273–297 (1995).
84. Breiman, L. Random Forests. *Mach. Learn* **45**, 5–32 (2001).
85. Prasad, A. M., Iverson, L. R. & Liaw, A. Newer classification and regression tree techniques: Bagging and random forests for ecological prediction. *Ecosystems* **9**, 181–199 (2006).
86. Huang, Z., Siwabessy, J., Nichol, S. L. & Brooke, B. P. Predictive mapping of seabed substrata using high-resolution multibeam sonar data: A case study from a shelf with complex geomorphology. *Mar. Geol.* **357**, 37–52 (2014).
87. Mutanga, O., Adam, E. & Cho, M. A. High density biomass estimation for wetland vegetation using WorldView-2 imagery and random forest regression algorithm. *Int. J. Appl. Earth Observation Geoinf.* **18**, 399–406 (2012).
88. Oliveira, S., Oehler, F., San-Miguel-Ayanz, J., Camia, A. & Pereira, J. M. C. Modeling spatial patterns of fire occurrence in Mediterranean Europe using Multiple Regression and Random Forest. *Ecol. Manag.* **275**, 117–129 (2012).
89. Heuvelink, G. B. M. Uncertainty quantification of GlobalSoilMap products. in *GlobalSoilMap: Basis of the global spatial soil information system*. (eds. D. Arrouays, N. McKenzie, J. Hempel, A. De Forges & A. McBratney) 335–340 (CRC Press, Boca Raton, 2014).
90. Arrouays, D. et al. Chapter Three - GlobalSoilMap: Toward a Fine-Resolution Global Grid of Soil Properties. *Advances in Agronomy*, **125**, 93–134 (2014).
91. Meyer, H., Reudenbach, C., Hengl, T., Katurji, M. & Nauss, T. Improving performance of spatio-temporal machine learning models using forward feature selection and target-oriented validation. *Environ. Model. Softw.* **101**, 1–9 (2018).
92. Roberts, D. R. et al. Cross-validation strategies for data with temporal, spatial, hierarchical, or phylogenetic structure. *Ecography* **40**, 913–929 (2017).
93. Ploton, P. et al. Spatial validation reveals poor predictive performance of large-scale ecological mapping models. *Nat. Commun.* **11**, 4540 (2020).
94. Meyer, H., Mila, C., Ludwig, M. & Linnenbrink, J. CAST: ‘caret’ applications for Spatial-Temporal Models. <https://github.com/HannaMeyer/CAST> (2023).
95. Meyer, H. & Pebesma, E. Machine learning-based global maps of ecological variables and the challenge of assessing them. *Nat. Commun.* **13**, 2208 (2022).
96. GEBCO Bathymetric Compilation Group. The GEBCO_2019 Grid - a continuous terrain model of the global oceans and land [Data Set]. <https://doi.org/10.5285/836f016a-33be-6ddc-e053-6c86abc0788e> (2019).
97. Itkin, M., König, M., Spreen, G. & Vongraven, D. Arctic Sea Ice Frequency with Maximum and Minimum Extent [Data set]. Norwegian Polar Institute. <https://doi.org/10.21334/npolar.2014.a89b2682> (2014).

Acknowledgements

This work was funded by the Norwegian seabed mapping programme Mareano. JK received support from the Research Council of Norway (grant # 332635).

Author contributions

M.D. conceptualization, data curation, formal analysis, investigation, methodology, project administration, validation, visualization, writing—original draft, writing—review & editing. S.P. data curation, writing—original draft, writing—review & editing. H.J. data curation, writing—original draft, writing—review & editing. T.T. funding acquisition, writing—original draft, writing—review & editing. L.R.B. funding acquisition, project administration, writing—original draft, writing—review & editing. J.K. writing—original draft, writing—review & editing.

Competing interests

The authors declare no competing interests.

Additional information

Supplementary information The online version contains supplementary material available at <https://doi.org/10.1038/s43247-024-01502-8>.

Correspondence and requests for materials should be addressed to Markus Diesing.

Peer review information *Communications Earth & Environment* thanks Ding He, Dorte Krause-Jensen and Tim Jennerjahn for their contribution to the peer review of this work. Primary Handling Editors: Mengze Li and Carolina Ortiz Guerrero. A peer review file is available.

Reprints and permissions information is available at <http://www.nature.com/reprints>

Publisher’s note Springer Nature remains neutral with regard to jurisdictional claims in published maps and institutional affiliations.

Open Access This article is licensed under a Creative Commons Attribution 4.0 International License, which permits use, sharing, adaptation, distribution and reproduction in any medium or format, as long as you give appropriate credit to the original author(s) and the source, provide a link to the Creative Commons licence, and indicate if changes were made. The images or other third party material in this article are included in the article's Creative Commons licence, unless indicated otherwise in a credit line to the material. If material is not included in the article's Creative Commons licence and your intended use is not permitted by statutory regulation or exceeds the permitted use, you will need to obtain permission directly from the copyright holder. To view a copy of this licence, visit <http://creativecommons.org/licenses/by/4.0/>.

© The Author(s) 2024